Nat Hazards (2017) 86:S203–S231
DOI 10.1007/s11069-016-2334-9

ORIGINAL PAPER

Stratigraphic features of the Maltese Archipelago: a synthesis

Niccolò Baldassini[1] · **Agata Di Stefano**[1]

Received: 15 December 2015 / Accepted: 19 April 2016 / Published online: 4 May 2016

Abstract The present study gathers a large amount of both existing and unpublished biostratigraphic data, which allows a detailed and complete definition of the stratigraphic features of the late Oligocene–late Miocene Maltese Archipelago sedimentary succession, recording in turn the tectonic and eustatic history of the Central Mediterranean region. We selected five sections in the Malta Island and three in Gozo, representative of the entire sedimentary succession, affected by well-known erosional surfaces, correlated to low-stands of the sea level, often associated with phoshatic layers, linked to the subsequent high-stands. The sedimentary interval, and thus the associated hiatuses, was constrained both by the biochronostratigraphic attribution and by the comparison with the third-order succession of the New Jersey passive margin, which shows strict analogy with the geodynamic context in which the Maltese succession deposited. The diachroneity at the base of the formations in the different sections, and the presence of intraformational unconformity/hiatuses, highlighted the role of the tectonic, which depicted a complex sedimentary basin, characterized by more distal versus more marginal sectors. Furthermore, the possibility to compare the sedimentary succession with the oxygen isotope curve connects the sedimentation interruptions, recorded within the Maltese Archipelago deposits, to global cooling events.

Keywords Maltese Archipelago succession · Late Oligocene–late Miocene · Calcareous plankton · Tectonics and eustatism

1 Introduction

The late Oligocene–Miocene time interval is characterized by a complex and dynamic climatic history mostly linked to ocean reorganization (Miller et al. 1991; Zachos et al. 2001, 2008), changes in organic carbon accumulation rates (Vincent and Berger 1985;

✉ Niccolò Baldassini
nbaldas@unict.it

[1] Dipartimento di Scienze Biologiche, Geologiche e Ambientali – Sezione di Scienze della Terra, Università di Catania, Corso Italia 57, 95129 Catania, Italy

Woodruff and Savin 1991; Holbourn et al. 2007), and orbital forcing (Zachos et al. 2001; Pälike et al. 2006; Holbourn et al. 2007; Mourik et al. 2011), which drove and influenced the sedimentary record. To be specific, Zachos et al. (2001) depicted a global shift toward cooler climate conditions (more pronounced since Serravallian) from the latest Oligocene to Pleistocene (Late Cenozoic Icehouse Mode of Kürschner et al. 2008), which is characterized by both warm intervals (Mid-Miocene Climatic Optimum of Woodruff and Savin 1989) and a series of glaciation events (Oi and Mi events; Miller et al. 1991, 1998; Pälike et al. 2006).

With the aim to depict these dynamics also in the Mediterranean area, we focused on the late Oligocene to late Miocene sedimentary succession outcropping on the Maltese islands, due to the bypass role across the Western and Eastern sectors of the basin, and to the spectacular outcrops of the successions. The study benefits from the numerous geological and stratigraphic researches performed through time on the deposits of the archipelago (Giannelli and Salvatorini 1972, 1975; Pedley et al. 1976; Pedley 1978; Mazzei 1986; Dart et al. 1993; Jacobs et al. 1996; Foresi et al. 2002, 2008, 2011, 2014; Sprovieri et al. 2002; John et al. 2003; Abels et al. 2005; Föllmi et al. 2008; Gruszczynski et al. 2008; Hilgen et al. 2009; Bianucci et al. 2011; Mourik et al. 2011; Baldassini et al. 2013; Baldassini and Di Stefano 2015).

In this paper, we consider all the existing biostratigraphic data gained through calcareous nannofossil and planktonic Foraminifera analyses, integrated with unpublished results (Di Stefano 1993; Baldassini 2012), with the aim of obtaining a detailed and complete bio-chronostratigraphic framework for the entire succession at both Malta and Gozo islands. For this purpose, key areas were selected, based on the optimal exposures, the completeness of the successions, and the availability of previous data. On the Malta Island, we focused on the southeastern, western (across the Victoria Line Fault), and northern outcrops, while at Gozo, on the southern and northern ones.

Furthermore, since the Maltese succession is affected by numerous depositional hiatuses associated to erosional surfaces at different stratigraphic levels, we attempted a comparison between the "normal" deposition intervals and the third-order sequences of the New Jersey passive margin (Miller et al. 1998; Steckler et al. 1999; Boulila et al. 2011) with the aim of chronostratigraphically constraining these sedimentary lacunas. Finally, we compared the recognized depositional phases, with the integrated oxygen isotope curve for the late Oligocene–late Miocene time interval (Kouwenhoven et al. 2003; Pekar and De Conto 2006; Boulila et al. 2011; Westerhold et al. 2011) to highlight the connection between climatic phases, eustatism, and depositional stages in the Maltese sedimentary succession.

2 The Maltese Archipelago in the geodynamic framework of Central Mediterranean

The Maltese islands occupy a central portion of the Mediterranean Sea, lying about 90 km south of Sicily and 350 km north of the Libyan coasts. The archipelago consists of three main islands, namely Malta, Gozo, and Comino (Fig. 1), and of numerous smaller islands.

From a geodynamic point of view, the Mediterranean area is mainly dominated by a ~N–S convergent tectonic context between the African and Eurasian plates that led to the subduction of the Tethyan oceanic crust below the neighboring continental plates (Gueguen et al. 1998; Carminati and Doglioni 2005) during the Cenozoic. The Maltese Archipelago, and specifically the Maltese Graben System, has been part of these strong

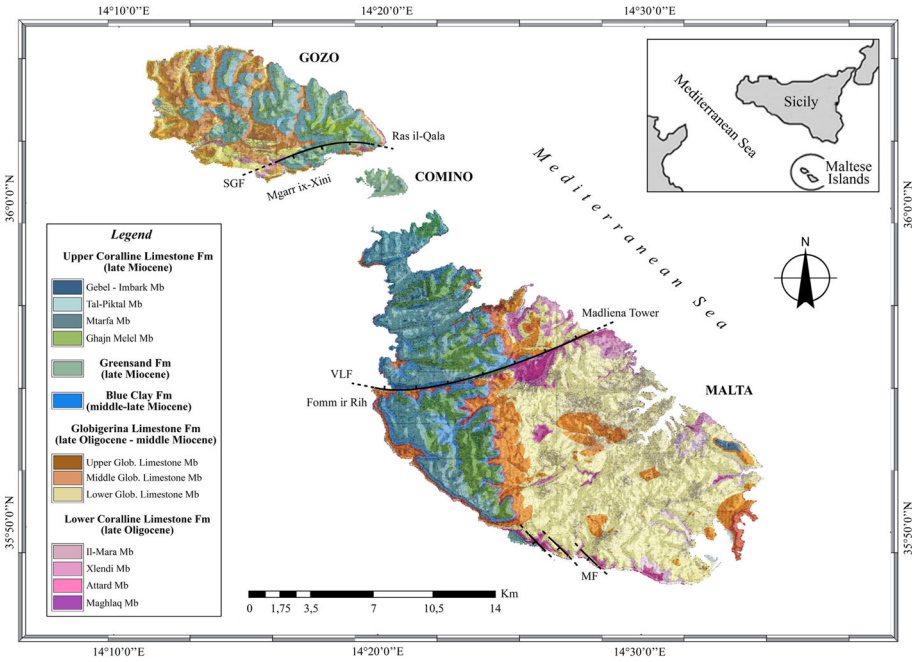

Fig. 1 Geological map of the Maltese Archipelago (Pedley 1993 modified). *VLF* Victoria Line Fault, *MF* Maghlaq Fault, *SGF* South Gozo Fault. The position of the Maltese island within the central Mediterranean is shown in the *inset*

tectonic modifications during the Neogene and Quaternary periods (Finetti 1984; Grasso and Pedley 1985; Grasso et al. 1985; Dart et al. 1993; Catalano et al. 2009; De Guidi et al. 2013; Cavallaro et al. 2016), representing the northeasternmost part of the Pantelleria Rift System in the foreland of the Appenine–Maghrebides fold-and-thrust belt.

The tectonic scenario characterizing the archipelago is represented by two different fault systems, which are widespread distributed throughout the whole Sicily Channel Rift Zone (Central-Western Mediterranean): the first, with an ENE–WSW trend, and the second displaying a NW–SE direction. According to Dart et al. (1993), the Maltese Graben System is the result of the coeval development of the two main rift trends (the NW–SE and the ENE–WSW trending normal faults), which occurred during the Neogene and reached their activity acme during the early Pliocene. Conversely, Corti et al. (2006) and Catalano et al. (2009) recognized a late Quaternary dextral strike-slip motion reactivation of the two systems of faults.

In this framework, the ENE–WSW trending faults are primarily represented by the Great Fault (also known as the Victoria Line Fault, VLF; Figs. 1, 2), which crosses the Malta Island from Fomm ir-Rih Bay (on the west) to Madliena Tower (on the northeast), giving rise northwards to a sequence of horsts and grabens, morphologically highlighted by alternation of ridges and valleys (Figs. 1, 2). The southern block of the Malta Island is affected by the secondary NW–SE faulting, mostly represented by the Maghlaq Fault (Figs. 1, 2).

The South Gozo Fault, roughly E–W oriented, crosses the homonymous island in its southernmost portion, from Mgarr ix-Xini (on the southwest) to Ras il-Qala (on the east) (Figs. 1, 2).

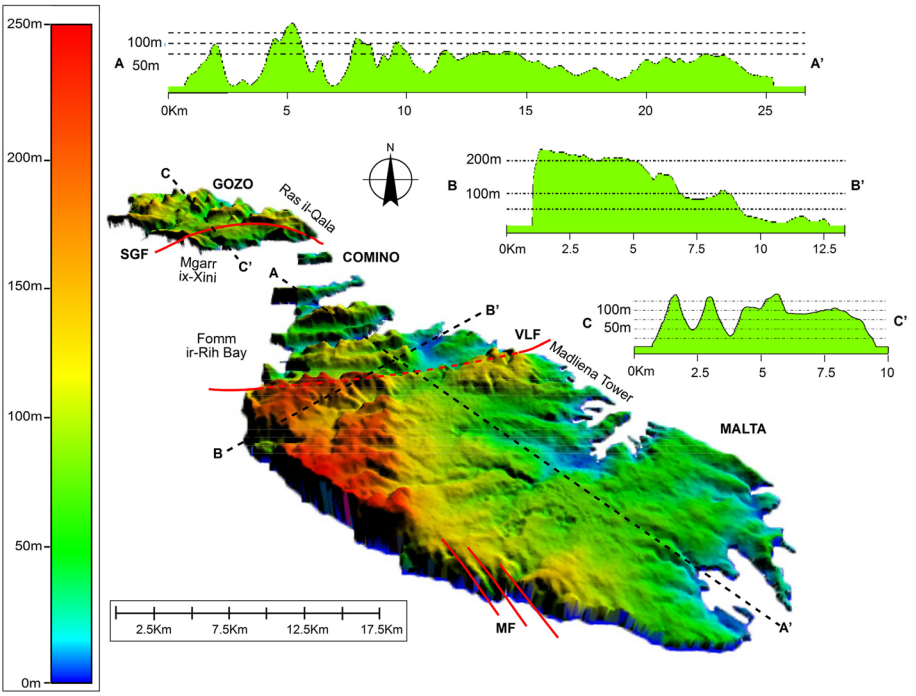

Fig. 2 Hill-shade digital elevation model (DEM) of the Maltese Archipelago showing the main morphological evidences

Tectonic activity played a key role in shaping the landscape of the Maltese Archipelago, triggering the occurrence of the highest elevations along the western coasts of the Malta and Gozo islands (sub-vertical cliffs increasing in height northwestwards) (Fig. 2), as a result of a northeastwards tilting, probably linked to the Pliocene uplift phase (Pedley 2011), which also led to the formation of a number of cut-back valleys. Conversely, low-lying coasts are widely distributed along the eastern and northeastern part of Malta (Biolchi et al. 2016) and the northern boundary of Gozo Island (Fig. 2).

3 Stratigraphic setting of the Maltese Archipelago

The Maltese sedimentary sequence consists of 5 formations covering the late Oligocene—early Messinian time span (Giannelli and Salvatorini 1972, 1975; Pedley 1978; Mazzei 1986; Di Stefano 1993; Pedley 1993; Foresi et al. 2002, 2008, 2011, 2014; Bianucci et al. 2011; Mourik et al. 2011; Baldassini 2012; Baldassini et al. 2013; Baldassini and Di Stefano 2015), which are in stratigraphic order, the Lower Coralline Limestone Formation (LCLF), the Globigerina Limestone Formation (GLF), the Blue Clay Formations (BCF), the Greensand Formation (GSF), and the Upper Coralline Limestone Formation (UCLF) (Fig. 1).

The LCLF (Fig. 3a) consists of late Oligocene (Chattian) (Giannelli and Salvatorini 1972; Felix 1973; Pedley 1976; Brandano et al. 2009a, b) shallow-marine bioclastic limestones (biosparites, biocalcarenites and biomicrites), yellowish to grayish in color, showing a maximum thickness of 140 m in outcrop (Pedley 1993) and of more than 650 m in boreholes (Pedley 1978). The formation has been subdivided into four members on the

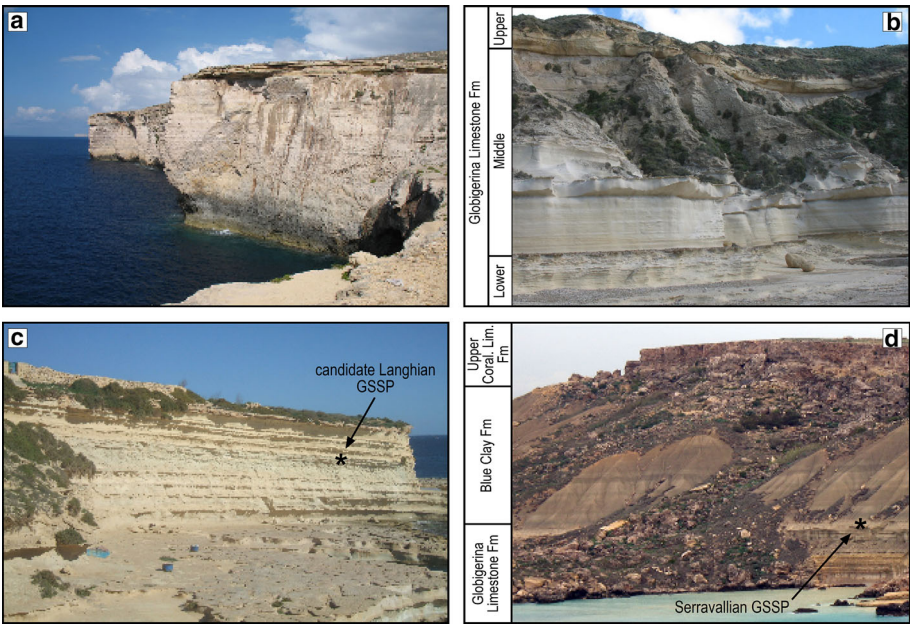

Fig. 3 Photographs of the formations widely outcropping in the Maltese Archipelago. **a** *Lower* Coralline Limestone Fm (Il Blata, Malta Island); **b** Globigerina Limestone Fm (Il Blata, Malta Island); **c** *Upper* Coralline Limestone Mb (St. Peter's Pool, Malta Island). The *asterisk* shows the stratigraphic position for the proposed section of the Langhian GSSP (Foresi et al. 2011); **d** Globigerina Limestone Fm, Blue Clay Fm, *Upper* Coralline limestone Fm outcropping at Ras il-Pellegrin (Malta Island). The *asterisk* shows the position of the Serravallian GSSP (Hilgen et al. 2009)

basis of the increasing grain size and the bioclastic content (Pedley 1978), which are from the older: Maghlak, Attard, Xlendi and Il-Mara. Fossils, represented by bivalves, gastropods, echinoids, brachiopods, corals, bryozoans, serpulids, corallinae algae and macroforaminifera, are widely distributed within the formation. The transition to the overlying GLF is marked by a phosphatized surface, reported by Carbone et al. (1987) as Basal Globigerina Limestone Phosphatic Bed.

The GLF (Fig. 3b) is late Oligocene (late Chattian) to middle Miocene (Langhian) in age (Giannelli and Salvatorini 1972; Di Stefano 1993; Foresi et al. 2008, 2011, 2014; Bianucci et al. 2011; Baldassini 2012; Baldassini et al. 2013; Baldassini and Di Stefano 2015) and represents the widest distributed formation in the archipelago, showing its maximum thickness (about 200 m) in the southeastern part of the Malta Island in the Delimara Peninsula (Baldassini et al. 2013; Foresi et al. 2011, 2014). The GLF generally consists of yellowish to grayish marly limestones subdivided, based on the occurrence of phosphoritic conglomerate beds (Pedley 1976; Rose et al. 1992; Baldassini and Di Stefano 2015), into the Lower (massive-bedded biomicrites and biomicrosparites, wackestones and packstones), Middle (marly biomicrites, mudstones and marly mudstones), and Upper (hard limestones, wackestones and subordinate calcareous marls and mudstones) Globigerina Limestone members (respectively, LGLM, MGLM, and UGLM, Fig. 3b). Two main phosphatic beds, between the lower and middle, and the middle and upper units, named by Rose et al. (1992) "Qammieh" and "Xwieni" conglomerate beds (QCB and XCB, respectively), are commonly accompanied by hiatal surfaces (Föllmi et al. 2008;

Gruszczynski et al. 2008). Recently Baldassini and Di Stefano (2015) recognized, along the western coast of the island of Malta, the occurrence of two more phosphorite-rich layers, defined as QCB1 and XCB1, respectively, within MGLM and UGLM.

The top of the LGLM is defined by the so-called Terminal Lower Globigerina Limestone Hardground (Gruszczynski et al. 2008), a weakly phosphatized, highly eroded and shaped surface, intensively penetrated by *Thalassinoides* burrows and showing a hummocky with convolute morphology.

The QCB, a 10–40 cm thick horizon unconformably overlying the LGLM, represents the base of the MGLM. It consists of sub-angular dark brown phosphatic pebbles and sub-rounded light brown phosphatized cobbles (maximum diameter of 15 cm) immersed in a whitish marly limestone matrix, with both phosphatized and non-phosphatized fossils (Baldassini and Di Stefano 2015 and reference therein). Glauconite occurs directly above the hardground surfaces as small sub-spherical pellets or as replacement of the micritic matrix (Pedley and Bennett 1985; Rose et al. 1992). The top of this bed is often planar due to marine erosion in a hardground environmental context, and the clasts are hardly cemented by polycyclic films of phosphate. The top of the MGLM is characterized by a highly bioturbated erosional surface ("Terminal Middle Globigerina Limestone Omissionground", Gruszczynski et al. 2008).

The XCB, a 10–30 cm thick horizon, unconformably overlying the intermediate member of the formation, defines the base of the UGLM. It is formed by phosphatic particles (about 1 mm in diameter) and sub-angular pebbles, immersed in a yellow-ochre limestone, with phosphatized and non-phosphatized fossils (Baldassini and Di Stefano 2015 and reference therein). The UGLM (Fig. 3b–d) is commonly represented by a lower layer represented by hard and compact brown-yellow limestones (wackestones), an intermediate ("Clay Rich Interval", John et al. 2003) consisting of gray calcareous marls (mudstones), and an upper formed by both marly layers and yellowish and strongly bioturbated limestones. The transition to the overlying formation is gradual and represented by a "Transitional Zone" (Felix 1973), characterized by a reduction in calcium carbonate and an increase in pelitic content. In the last 40 cm (Fig. 4a), this interval exhibits small grains of glauconite (Fig. 4b, c), phosphatic particles (Fig. 4d, e), and traces of oxidation.

The BCF (Fig. 3d) consists of Serravallian–Tortonian (Felix 1973; Giannelli and Salvatorini 1975; Mazzei 1986; Di Stefano 1993; Sprovieri et al. 2002; Bianucci et al. 2011; Baldassini 2012) blue-gray marly clays showing maximum thickness of 75 m (Pedley 1993). A light gray glauconitic sand layer, 1–2 m thick, with abundant fossil content (mainly represented by *Flabellipecten* and *Amusium*) unconformably occurs in the uppermost part, about 3–7 m below the overlying GSF (Giannelli and Salvatorini 1975). According to Pedley (1978), the uppermost part of the BCF consists of deposits transported eastward as the result of erosive phenomena on structural highs west and north of the archipelago.

The late Neogene (middle Tortonian; Bianucci et al. 2011) marly-clayey sands and arenites (bioclastic wackestones), rich in grains of glauconite, belonging to the GSF are poorly represented in the archipelago, showing its maximum thickness (11 m according to Pedley 1993) in the central part of Gozo Island. The fossiliferous content is mostly represented by mollusks, gastropods, brachiopods, echinoids, bryozoans, algae, shark teeth, and other remains of marine vertebrates.

The youngest Miocene deposits of the Maltese sedimentary succession belongs to the UCLF (Fig. 3d) and has been attributed to the late Tortonian to pre-evaporitic Messinian (late Miocene) (Giannelli and Salvatorini 1975; Russo and Bossio 1975; Mazzei 1986;

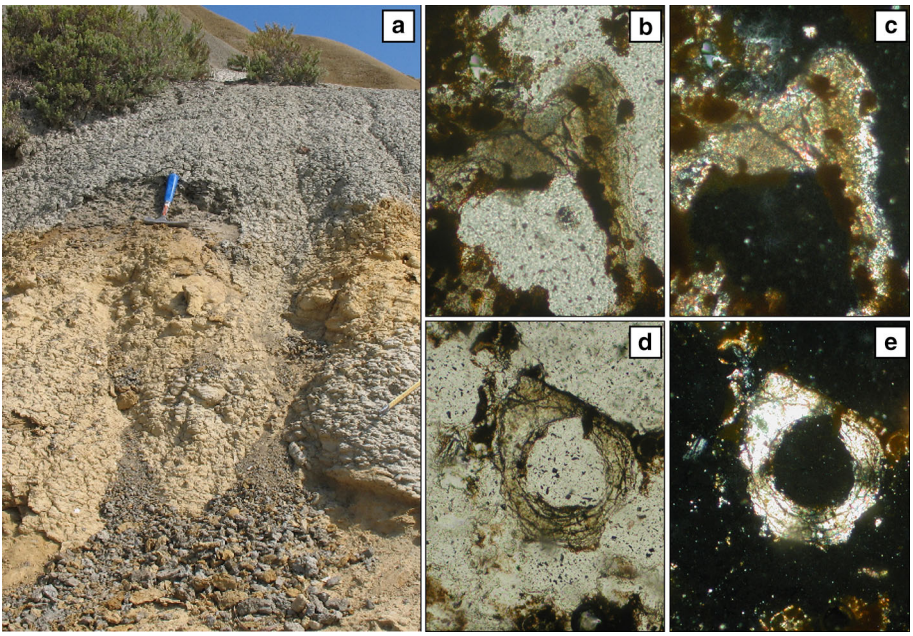

Fig. 4 **a** Transition between the Globigerina Limestone and Blue Clay formations in the Xatt L-Ahmar outcrop (Gozo Island). **b**, **c** Photomicrographs under plane and cross polarized light (×40 magnification) of glauconite overgrowth; **d**, **e** phosphatic ring-like structure within the bed under plane and polarized light (×40 magnification)

Bianucci et al. 2011; Pedley 2011). The formation, which is characterized by a maximum thickness of about 50 m (Pedley 1993), almost exclusively consists of fossiliferous limestones, where coralline algae are the principal component. According to Pedley (1976, 1978), the formations are subdivided into four members, which are from the older to the younger: the Ghajn Melel, Mtarfa, Tal-Piktal, and Gebel Imbark.

4 Biostratigraphic framework of the Maltese sedimentary succession

The wide available biostratigraphic data, both based on nannofossils and Foraminifera, concerning the Maltese succession (Giannelli and Salvatorini 1972, 1975; Mazzei 1986; Di Stefano 1993; Kienel et al. 1995; Foresi et al. 2002, 2008, 2011, 2014; Hilgen et al. 2009; Bianucci et al. 2011; Mourik et al. 2011; Baldassini 2012; Baldassini et al. 2013; Baldassini and Di Stefano 2015) offer a thorough and highly detailed biostratigraphic framework for the Oligo–Miocene deposition of the archipelago. To provide a synthesis of the large amount of data, in some cases scattered, five study areas were selected on Malta Island (Table 1), located in the southeastern coast (Delimara section), along the western coast across the Victoria Line Fault (Il Blata, Fomm ir-Rih Bay and Karraba sections), and in the northern part (Qammieh section). Similarly, three study areas were chosen on the Gozo Island (Table 1), respectively, situated along the southern coast (Xatt L-Ahmar section),and in the northern sector (Dabrani and Xwieni Bay sections).

Table 1 List of the considered outcrops both in Malta and Gozo islands

Section	Geographic position and coordinates		Lithostratigraphy	Authors
Delimara	SE Malta Island	35°52′02.01″N 14°34′25.35″E	II-Mara Mb (LCLF)	Baldassini et al. (2013)
			Lower Globigerina Limestone Mb (GLF)	
		35°50′26.87″N 14°33′41.36″E	Middle Globigerina Limestone Mb (GLF)	Foresi et al. (2014)
		35°49′59.82″N 14°33′44.53″E	Upper Globigerina Limestone Mb (GLF)	Foresi et al. (2011)
II Blata	W Malta Island	35°53′52.38″N 14°19′48.66″E	II-Mara Mb (LCLF)	Baldassini et al. (2013); Baldassini and Di Stefano (2015)
			Globigerina Limestone Fm	
Fomm ir-Rih Bay	W Malta Island	35°54′53.05″N 14°20′09.40″E	Middle Globigerina Limestone Mb (GLF)	Giannelli and Salvatorini (1972, 1975); Mazzei (1986); Di Stefano (PhD); Foresi et al. (2002); Hilgen et al. (2009); Mourik et al. (2011)
			Upper Globigerina Limestone Mb (GLF)	
			Blue Clay Fm	
			Greensand Fm	
			Mtarfa Mb (UCLF)	
			Tal-Piktal Mb (UCLF)	
Karraba	W Malta Island	35°55′34.32″N 14°20′38.89″E	Upper Globigerina Limestone Mb (GLF)	Giannelli and Salvatorini (1975); Di Stefano (PhD)
			Blue Clay Fm	
			Greensand Fm	
			Mtarfa Mb (UCLF)	
			Tal-Piktal Mb (UCLF)	
Qammieh	N Malta Island	35°58′11.43″N 14°19′25.22″E	Xlendi Mb (LCLF)	Baldassini et al. (2013); Baldassini and Di Stefano (2015)
			Globigerina Limestone Fm	
Xatt L-Ahmar	S Gozo Island	36°01′11.00″N 14°17′26.43″E	Globigerina Limestone Fm	Baldassini (PhD)
			Blue Clay Fm	

Table 1 continued

Section	Geographic position and coordinates		Lithostratigraphy	Authors
Dabrani	N Gozo Island	36°03′47.72″N 14°14′47.48″E	Xlendi Mb (LCLF) Globigerina Limestone Fm Blue Clay Fm Greensand Fm Ghajn Melel Mb (UCLF) Tal-Piktal Mb (UCLF)	Giannelli and Salvatorini (1972, 1975); Mazzei (1986); Di Stefano (PhD); Baldassini et al. (2013)
Xwieni Bay	N Gozo Island	36°04′42.37″N 14°14′56.45″E	Xlendi Mb (LCLF) Globigerina Limestone Fm Blue Clay Fm Greensand Fm Ghajn Melel Mb (UCLF) Tal-Piktal Mb (UCLF)	Giannelli and Salvatorini (1972, 1975); Mazzei (1986); Di Stefano (PhD); Kienel et al. (1995); Mourik et al. (2011); Baldassini (PhD); Baldassini et al. (2013)

For each section, the main lithostratigraphic features and the relative references are reported

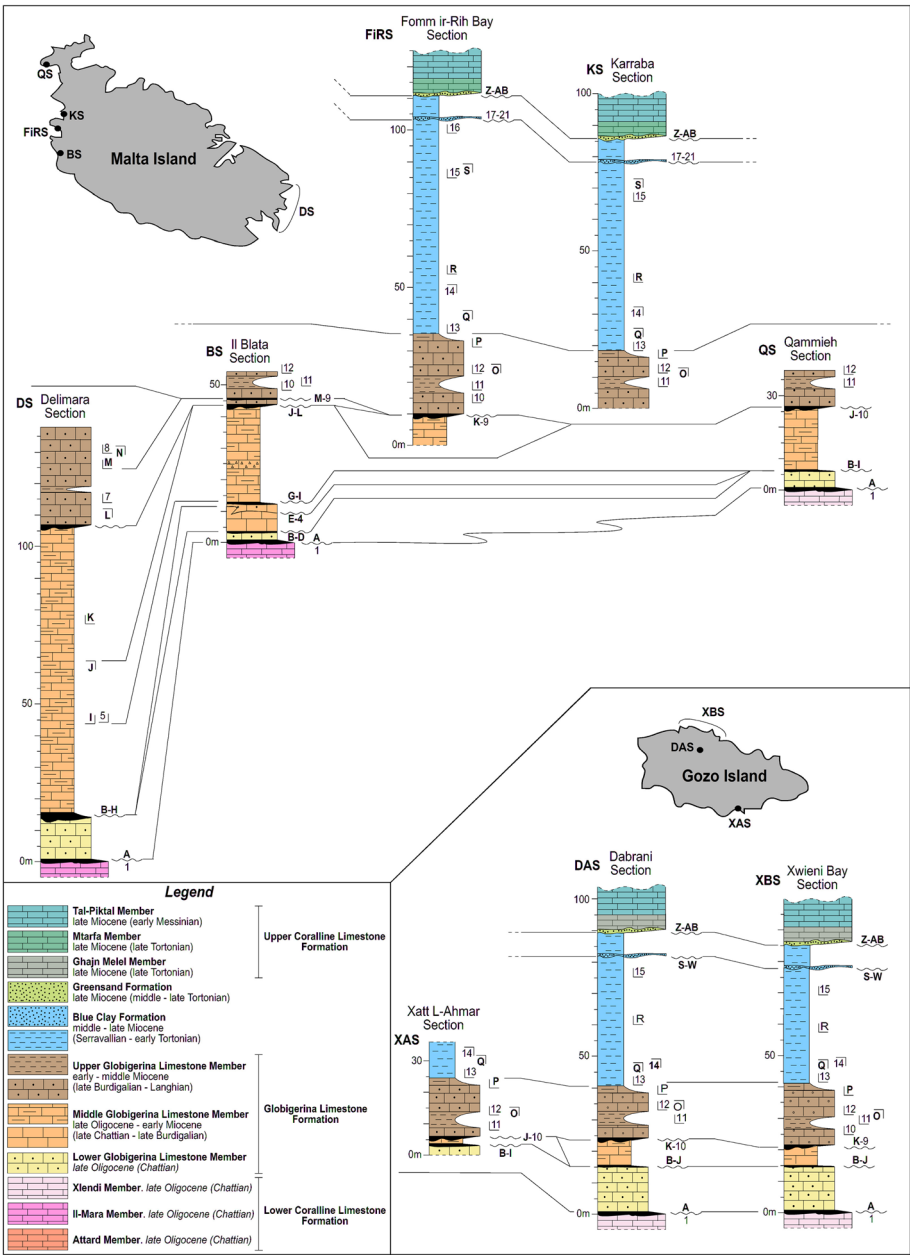

Fig. 5 Biostratigraphic (calcareous nannofossil and planktonic Foraminifera) correlation between the considered sections on Malta and Gozo islands. On each map is shown the geographic position of the outcrops. *Numbers* (nannofossils) and *letters* (Foraminifera) refer to the biostratigraphic events listed in Tables 2 and 3

4.1 Lower Coralline Limestone Formation

Brandano et al. (2009a, b), considering the occurrence and distribution of the skeletal components of photozoans and heterozoans, framed the deposition of the LCLF, and specifically of the Attard Member, to the Chattian Stage (late Oligocene), in agreement with the attribution of the entire formation to the same time interval reported by the Geological Map of the Maltese Islands (Pedley 1993). Despite the very poor occurrence of planktonic Foraminifera and the absence of calcareous nannofossils due to the shallow depositional environment, the heteropic deposits belonging to the Xlendi Member (Qammieh, Dabrani and Xwieni Bay sections) and to the Il-Mara Member (Il Blata and Delimara sections) (Figs. 3a, 5; Table 1) can be indirectly framed at least to the lower part of the MNP25a Zone of Fornaciari and Rio (1996) and to the P22 Zone of Blow (1969) (Fig. 6).

4.2 Globigerina Limestone Formation

The GLF ranges in the whole from late Oligocene to Langhian (Giannelli and Salvatorini 1972; Mazzei 1986; Foresi et al. 2011, 2014; Baldassini et al. 2013; Baldassini and Di Stefano 2015). In all the considered outcrops (Table 1), both in Malta and Gozo islands, the LGLM is ascribable to the upper part of the MNP25a and P22 zones (Figs. 5, 6; Tables 2, 3) and thus to the late Chattian (late Oligocene) (Giannelli and Salvatorini 1972; Mazzei 1986; Baldassini et al. 2013; Baldassini and Di Stefano 2015). The attribution is supported by the presence of *Sphenolithus ciperoensis* within the calcareous nannofossils, and by the occurrence of *Paragloborotalia opima* and the absence of *P. kugleri* (the first occurrence of this latter taxon approximates the Global Stratigraphic Section and Point of the Aquitanian stage and thus of the Neogene Period; Steininger et al. 1997) as concerns the planktonic Foraminifera.

The oldest deposits belonging to the MGLM were recognized by Baldassini and Di Stefano (2015) at Il Blata (Malta Island) (Fig. 3b). The authors documented a latest Oligocene age, ascribing these deposits within the nannofossil MNN1b Subzone based on the presence of *Sphenolithus delphix* (zonal nominal taxon). This attribution is confirmed also by the planktonic Foraminifera assemblages, which are still indicative of the P22 Zone, due to the absence of the *P. kugleri* specimens (Figs. 5, 6; Tables 2, 3). At Il Blata section (Fig. 3b), the same authors also recognized an interval of deposition ascribable to the upper portion of the MNN1d, late Aquitanian in age (Figs. 5, 6; Tables 2, 3), based on the lowest percentages of *Helicosphaera carteri* compared to those of *H. euphratis*, and on the absence of *H. ampliaperta* whose first occurrence defines the base of the following biozone (Table 3). Furthermore, this attribution is supported by the recognition of the lower–middle part of the foraminiferal MMi2b Subzone of Foresi et al. (2014), due to the presence of *Globigerinoides altiaperturus* (whose first occurrence defines the base of the subzone; Table 2), and randomly coiled specimens of *Paragloborotalia acrostoma* (the increase of sinistral forms defines the beginning of the following subzone; Table 2).

Although most of the MGLM is Burdigalian (early Miocene), different age intervals were recognized throughout the archipelago (Figs. 5, 6). In the Delimara section, where the member shows its maximum thickness, Foresi et al. (2014) documented an early to middle Burdigalian age, by recognizing the calcareous nannofossil MNN2b (Fornaciari and Rio 1996)—MNN4a (Di Stefano et al. 2008) interval on the basis of the first occurrence of *Sphenolithus belemnos* (which defines the basis of the MNN3a Zone; Table 3) and of the

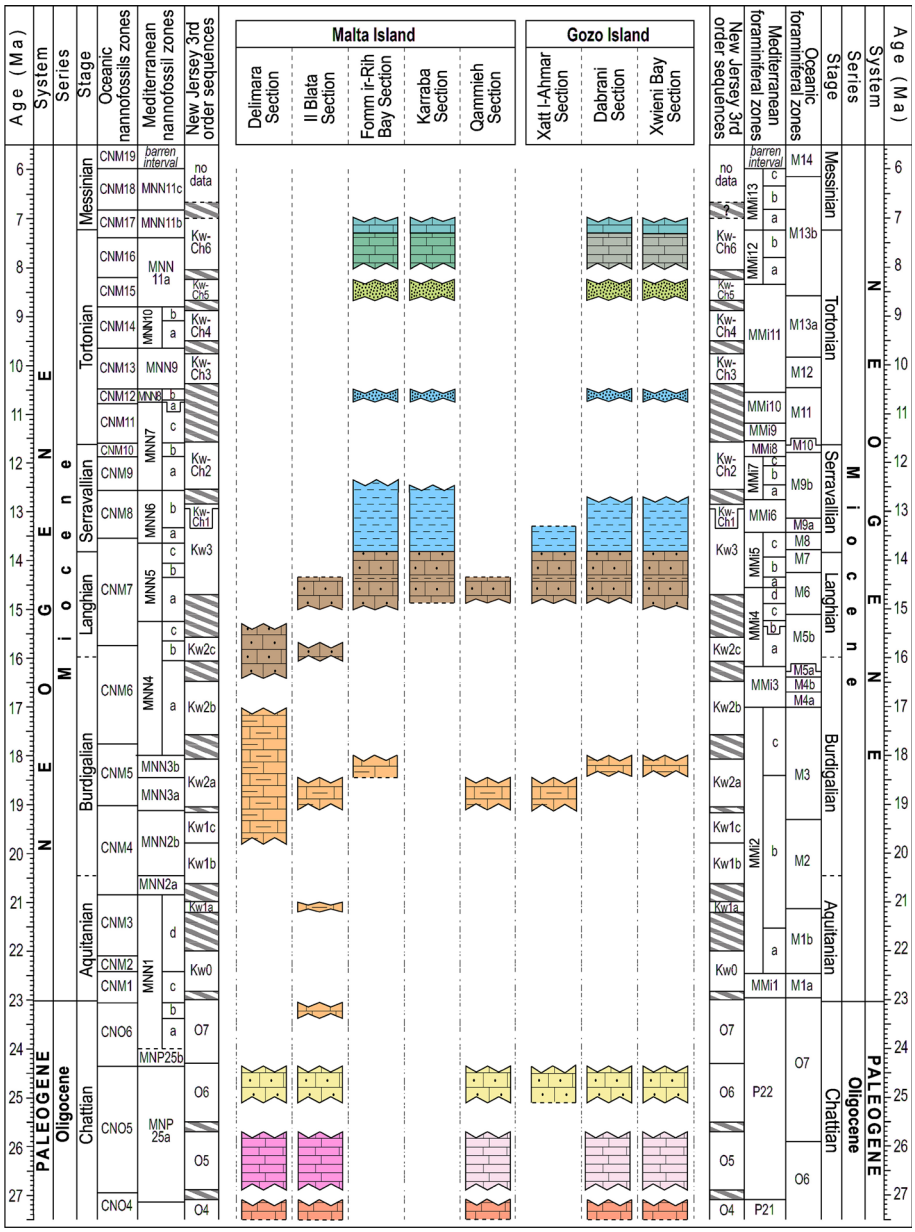

common presence of *S. heteromorphus* (its first common occurrence defines the base of the MNN4a Subzone; Table 3) and *H. ampliaperta* (its last common occurrence marks the base of the MNN4b Subzone), respectively, in lower and upper part of the section. Regarding the planktonic Foraminifera, Foresi et al. (2014) recognized the MMi2b–MMi2c interval zones by identifying, in the lower layers the presence of *G. altiaperturus* and the first common occurrence of *P. acrostoma*, and in the middle layers, high abundance of sinistral coiled *P. acrostoma* (the acme base of the sinistral specimens defines the base of

◀**Fig. 6** Bio-chronostratigraphic framework adopted for the present this study. The depositional intervals recognized on Malta and Gozo islands are compared to the Oligo–Miocene third-order sequences of Boulila et al. (2011). The Oceanic nannofossil zonation includes Backman et al. (2012) and Agnini et al. (2014); the Mediterranean nannofossil zonation includes Fornaciari and Rio (1996), Sprovieri et al. (2002), Raffi et al. (2003) and Iaccarino et al. (2011). Bioevents chronology from: Sprovieri et al. (2002), Abdul Aziz et al. (2008), Turco et al. (2011), Backman et al. (2012), Agnini et al. (2014) and Foresi et al. (2014). The Oceanic foraminiferal zonation includes Wade et al. (2011); the Mediterranean foraminiferal zonation includes Berggren et al. (1995), Iaccarino et al. (2007, 2011), Foresi et al. (2014). Bioevents chronology from: Berggren et al. (1995), Steininger and Iaccarino (1996), Sprovieri et al. (1999), Lourens et al. (2004), Huesing et al. (2007), Abdul Aziz et al. (2008), Turco et al. (2011), Wade et al. (2011), Foresi et al. (2014)

the MMi2b Subzone of Foresi et al. 2014; Table 2). The deposits of the member outcropping at Il Blata, Qammieh, and Xatt L-Ahmar sections (Figs. 5, 6) were ascribed to the middle Burdigalian nannofossil MNN3a Zone (Mazzei 1986; Di Stefano 1993; Baldassini 2012; Baldassini and Di Stefano 2015) and to the planktonic Foraminifera MMi2b Subzone (Giannelli and Salvatorini 1972), respectively, on the basis of (Tables 2, 3) the common presence of *S. belemnos*, and of the occurrence of *G. altiaperturus*. In the northern sector of Gozo (Dabrani and Xwieni Bay sections) and in the Fomm ir-Rih section, the very low percentages of *S. belemnos* and the acme base of the sinistral *P. acrostoma* allowed to recognize the MNN3b Zone of Fornaciari and Rio (1996) and the MMi2c Subzone of Foresi et al. (2014), respectively (Figs. 5, 6; Tables 2, 3).

The UGLM crops out with its oldest deposits in the southeastern sector of the Malta Island (Delimara section), where Foresi et al. (2011) recognized the MNN4a–MNN5a (calcareous nannofossils) and the MMi3–MMi4c (planktonic Foraminifera) zonal intervals (Di Stefano et al. 2008; Iaccarino et al. 2011), attributable to the late Burdigalian–early Langhian time interval (Figs. 3c, 5, 6). This bio-chronostratigraphic reference, as regards the calcareous nannofossils, was justified through the recognition of the last common occurrence of *H. ampliaperta* in the lowermost meters of the section and the end of the paracme of *Sphenolithus heteromorphus* in the uppermost layers (Figs. 5, 6; Tables 2, 3). Concerning the planktonic Foraminifera, Foresi et al. (2011) recognized the first occurrences of *Globigerinoides sicanus* and *Paragloborotalia glomerosa curva* (Table 2), respectively, in the lower and topmost layers of the section. Baldassini and Di Stefano (2015) recognized a similar interval of deposition in the section of Il Blata (Figs. 5, 6) that has been ascribed to the early Langhian MNN4b Subzone of Di Stefano et al. (2008) because of the discontinuous occurrence of *H. ampliaperta* and the abundant distribution of *S. heteromorphus* (Table 3). In other outcrops in Malta and Gozo, sediments of the UGLM (Fig. 3b–d) are mainly of Langhian age (Figs. 5, 6). The interval between the MNN5a and MNN5c (Di Stefano et al. 2008) nannofossil zones was detected at Il Blata, Fomm ir-Rih, Karraba, and Qammieh (Malta), and Xatt L-Ahmar, Dabrani, and Xwieni Bay (Gozo) (references in Table 1), mostly based on the common distribution of *S. heteromorphus* since the base and the first common occurrence of *Helicosphaera walbersdorfensis* in the younger layers (Table 3). A greater biostratigraphic detail is offered by the analyses of the planktonic Foraminifera assemblages, which allowed the ascription of the member to the MMi4c–MMi5b (Iaccarino and Salvatorini 1982; Di Stefano et al. 2008) interval zones at Il Blata and Fomm ir-Rih Bay (Hilgen et al. 2009), and along the northern coast of Gozo Island, in the Xwieni Bay section. This attribution is supported by the recognition of the first occurrences of *Paragloborotalia glomerosa circularis* and *Orbulina universa*, respectively, in the lower and middle-upper part of the considered sections (Figs. 5, 6; Table 2). The sections of Karraba, Qammieh, Xatt L-Ahmar, and Dabrani, respectively, outcropping along the northern part of Malta Island and in the southern and northern part of

Table 2 List of the zonal planktonic Foraminifera bioevents used in the present study, with relative ages and references

Basal marker			Biozone	Author	Age (Ma)	Author (age)
26	S/D	*N. acostaensis*	MMi13c	Iaccarino et al. (2007)	6.35	Lourens et al. (2004)
25	FO	*G. nicolae*	MMi13b	Iaccarino et al. (2007)	6.83	Lourens et al. (2004)
24	FCO	*G. miotumida* gr.	MMi13a	Iaccarino et al. (2007)	7.24	Lourens et al. (2004)
23	FO	*G. suterae*	MMi12b	Iaccarino et al. (2007)	7.81	Sprovieri et al. (1999)
22	FO	*G. extremus*	MMi12a	Iaccarino et al. (2007)	8.35	Sprovieri et al. (1999)
21	FRO	*N. acostaensis* s.s.	MMi11	Iaccarino et al. (2007)	10.57	Huesing et al. (2007)
20	LO	*P. siakensis*	MMi10	Iaccarino et al. (2007)	11.20	Huesing et al. (2007)
19	LCO	*G. subquadratus*	MMi9	Iaccarino et al. (2007)	11.56	Lourens et al. (2004)
18	FO	*N. atlantica preatlantica*	MMi8	Iaccarino et al. (2007)	11.78	Lourens et al. (2004)
17	LO	*P. mayeri*	MMi7c	Iaccarino et al. (2007)	12.07	Lourens et al. (2004)
16	FCO	*P. mayeri*	MMi7b	Iaccarino et al. (2007)	12.43	Lourens et al. (2004)
15	FO	*P. partimlabiata*	MMi7a	Iaccarino et al. (2007)	12.77	Lourens et al. (2004)
14	LO	*G. peripheroronda*	MMi6	Iaccarino et al. (2011)	13.41	Abdul Aziz et al. (2008)
13	FO	*G. praemenardii*	MMi5c	Iaccarino et al. (2011)	13.92	Abdul Aziz et al. (2008)
12	FO	*O. universa*	MMi5b	Iaccarino et al. (2011)	14.36	Abdul Aziz et al. (2008)
11	FO	*O. suturalis*	MMi5a	Iaccarino et al. (2011)	14.56	Abdul Aziz et al. (2008)
10	FO	*P. gl. circularis*	MMi4d	Iaccarino et al. (2011)	14.89	Abdul Aziz et al. (2008)
9	FO	*P. gl. curva*	MMi4c	Iaccarino et al. (2011)	15.23	Turco et al. (2011)
8	AaB	*P. siakensis*	MMi4b	Iaccarino et al. (2011)	15.36	Turco et al. (2011)
7	FO	*G. sicanus* (3 apertures)	MMi4a	Iaccarino et al. (2011)	16.18	Turco et al. (2011)
6	LO	*C. dissimilis*	MMi3	Iaccarino et al. (2007)	17.00	Di Stefano et al. (2011)
5	AB-r/s	*P. acrostoma*	MMi2c	Foresi et al. (2014)	18.40	Foresi et al. (2014)
4	FO	*G. altiaperturus*	MMi2b	Iaccarino et al. (2007)	21.12	Steininger and Iaccarino (1996)
3	FO	*G. dehiscens*	MMi2a	Iaccarino et al. (2007)	22.44	Wade et al. (2011)
2	FO	*P. kugleri*	MMi1	Iaccarino et al. (2007)	22.96	Lourens et al. (2004)
1	LO	*P. opima*	P22	Berggren et al. (1995)	27.10	Berggren et al. (1995)

LO last occurrence, *LCO* last common occurrence, *FO* first occurrence, *FCO* first common occurrence, *FRO* first regular occurrence, *AB-r/s* acme base and coiling change from random to sinistral, *AaB* acme a base, *S/D* coiling change from sinistral to dextral

Table 3 List of the zonal calcareous nannofossil bioevents used in the present study, with relative ages and references

Basal marker			Biozone	Author	Age (Ma)	Author (age)
AD	FO	*N. amplificus*	MNN11c	Raffi et al. (2003)	6.82	Backman et al. (2012)
AC	FO	*A. primus*	MNN11b	Raffi et al. (2003)	7.39	Backman et al. (2012)
AB	PB	*R. pseudoumbilicus*	MNN11a	Raffi et al. (2003)	8.80	Backman et al. (2012)
AA	FCO	*D. pentaradiatus*	MNN10b	Raffi et al. (2003)	9.15	Backman et al. (2012)
Z	LO	*D. hamatus*	MNN10a	Raffi et al. (2003)	9.65	Backman et al. (2012)
Y	FO	*D. bellus* gr.	MNN9	Raffi et al. (2003)	10.49	Backman et al. (2012)
X	FCO	*H. stalis*	MNN8b	Sprovieri et al. (2002)	10.71	Sprovieri et al. (2002)
W	LO	*H. walbersdorfensis*	MNN8a	Sprovieri et al. (2002)	10.76	Sprovieri et al. (2002)
U	LCO	*D. kugleri*	MNN7c	Sprovieri et al. (2002)	11.60	Sprovieri et al. (2002)
T	FCO	*D. kugleri*	MNN7b	Sprovieri et al. (2002)	11.90	Sprovieri et al. (2002)
S	LCO	*C. premacintyrei*	MNN7a	Sprovieri et al. (2002)	12.51	Sprovieri et al. (2002)
R	FCO	*R. pseudoumbilicus* > 7 μm	MNN6b	Sprovieri et al. (2002)	13.32	Sprovieri et al. (2002)
Q	LO	S. *heteromorphus*	MNN6a	Sprovieri et al. (2002)	13.59	Sprovieri et al. (2002)
P	FCO	*H. walbersdorfensis*	MNN5c	Iaccarino et al. (2011)	14.05	Abdul Aziz et al. (2008)
O	LCO	*H. waltrans*	MNN5b	Iaccarino et al. (2011)	14.35	Abdul Aziz et al. (2008)
N	PE	*S. heteromorphus*	MNN5a	Iaccarino et al. (2011)	15.26	Turco et al. (2011)
M	PB	*S. heteromorphus*	MNN4c	Iaccarino et al. (2011)	15.64	Turco et al. (2011)
L	LCO	*H. ampliaperta*	MNN4b	Iaccarino et al. (2011)	16.05	Turco et al. (2011)
K	FCO	*S. heteromorphus*	MNN4a	Fornaciari and Rio (1996)	17.99	Foresi et al. (2014)
J	LCO	*S. belemnos*	MNN3b	Fornaciari and Rio (1996)	18.44	Foresi et al. (2014)
I	FO	*S. belemnos*	MNN3a	Fornaciari and Rio (1996)	19.12	Foresi et al. (2014)
H	FO	*H. ampliaperta*	MNN2b	Fornaciari and Rio (1996)	20.43	Backman et al. (2012)
G	AE	*H. euphratis*	MNN2a	Fornaciari and Rio (1996)	20.89	Backman et al. (2012)
F	FO	*S. disbelemnos*	MNN1d	Fornaciari and Rio (1996)	22.41	Backman et al. (2012)
E	LO	*S. delphix*	MNN1c	Fornaciari and Rio (1996)	23.06	Backman et al. (2012)

Table 3 continued

Basal marker			Biozone	Author	Age (Ma)	Author (age)
D	FO	*S. delphix*	MNN1b	Fornaciari and Rio (1996)	23.38	Backman et al. (2012)
C	LCO	*D. bisectus*	MNN1a	Fornaciari and Rio (1996)	No data	
B	LO	*S. ciperoensis*	MNP25b	Fornaciari and Rio (1996)	24.36	Agnini et al. (2014)
A	FO	*S. ciperoensis*	MNP25a	Fornaciari and Rio (1996)	27.14	Agnini et al. (2014)

LO last occurrence, *LCO* last common occurrence, *FO* first occurrence, *FCO* first common occurrence, *AE* acme end, *PB* paracme beginning, *PE* paracme end

Gozo Island, are characterized by younger basal levels, which have been ascribed to the MMi4d–MMi5b interval zones of Iaccarino and Salvatorini (1982) through the recognition from the base of *P. glomerosa circularis* specimens (Figs. 5, 6; Table 2).

4.3 Blue Clay Formation

The BCF conformably follows the GLF through a transitional interval that hosts, at its top, the GSSP of the Serravallian stage dated at 13.82 Ma (Hilgen et al. 2009; Figs. 3d, 4). From the base up to the unconformity below the sandy bed in the uppermost portion (Fig. 5), it is characterized by a depositional interval wider at Malta than at Gozo. Specifically, in Fomm ir-Rih Bay and Karraba sections the succession can be ascribed to the nannofossil MNN5c–MNN7a (Di Stefano et al. 2008; Sprovieri et al. 2002) zones (Mazzei 1986; Di Stefano 1993; Foresi et al. 2002; Hilgen et al. 2009; Mourik et al. 2011), while at Dabrani and Xwieni Bay sections, to the MNN5c–MNN6b (Mazzei 1986; Di Stefano 1993; Mourik et al. 2011) (Figs. 5, 6). This biostratigraphic attribution is supported by the common presence from the base of the species *H. walbersdorfensis*, and by the last common occurrence of *Calcidiscus premacintyrei*, which is observable only in the Maltese outcrops (Figs. 5, 6; Table 3). The planktonic Foraminifera content allowed to further refine the biostratigraphic data, highlighting a slightly wider depositional interval at Fomm ir-Rih Bay (MMi5c–MMi7b of Sprovieri et al. 2002) in comparison with Karraba, Dabrani, and Xwieni Bay (MMi5c–MMi7a) (Figs. 5, 6; Giannelli and Salvatorini 1975; Foresi et al. 2002; Hilgen et al. 2003; Mourik et al. 2011). These biostratigraphical attributions are based on the first occurrence of *Globorotalia praemenardii* (that slightly predates the GSSP of the Serravallian stage at the base of the formation), and the first common occurrence of *Paragloborotalia mayeri*, which is only recorded in the uppermost layers of Fomm ir-Rih Bay section (Figs. 5, 6; Table 2).

The glauconite-rich deposits of the BCF, sandwiched between the sandy bed and the overlying GSF (Fig. 5), and outcropping at Fomm ir-Rih Bay, Karraba, Dabrani, and Xwieni Bay sections, were attributed by Bianucci et al. (2011) to the middle Tortonian (late Miocene) nannofossil MNN8a–MNN8b zones of Fornaciari et al. (1996), and by Giannelli and Salvatorini (1975) and Cita et al. (1979) to the MMi10–MMi11 Foraminifera zones of Iaccarino et al. (2007) (Figs. 5, 6). These biostratigraphic attributions are supported, respectively, by the recognition of the last occurrence of *H. walbersdorfensis* (boundary between the MNN8a and MNN8b subzones) and by the regular occurrence of *Neogloboquadrina acostaensis* (Tables 2, 3).

4.4 Greensand and Upper Coralline Limestone Formations

Due to the shallow-water depositional environment characterizing the GSF and the UGLF (Pedley and Waugh 1976), the biostratigraphic attribution of these deposits through calcareous nannofossil and planktonic Foraminifera assemblages has been difficult. Mazzei (1986) and Kienel et al. (1995) documented both in Malta (Fomm ir-Rih Bay and Karraba sections) and Gozo (Dabrani and Xwieni Bay sections) a latest Tortonian to early Messinian deposition, through the recognition of the nannofossil CN9b Subzone of Okada and Bukry (1980), which roughly corresponds to the MNN11b–MNN11c of Raffi et al. (2003) (Figs. 5, 6). Furthermore, Giannelli and Salvatorini (1975) ascribed the same deposits to the planktonic Foraminifera MMi12b–MMi13c. Recently, Bianucci et al. (2011) better framed the deposition of the GSF to the nannofossil MNN11a Zone (Figs. 5, 6), which is in

agreement with the age obtained for these deposits by Föllmi et al. (2008) through the Strontium isotopes dating.

The nannofossil and Foraminifera data, respectively, obtained by Mazzei (1986) and Kienel et al. (1995), and by Giannelli and Salvatorini (1975), can be referred only to the UCLF. This interpretation is supported by Bianucci et al. (2011) who highlighted, for the lower part of the formation, the MNN11a Zone, not excluding the presence of the subsequent MNN11b.

5 Chronostratigraphic frame of the depositional intervals of the Maltese sedimentary succession

The occurrence of erosional surfaces, often associated to autochthonous phosphatization and followed, mostly in the GLF, by allochthonous phosphatic pebbles and cobbles accumulations, has been associated with the development of sedimentary hiatuses of different duration throughout the archipelago (Föllmi et al. 2008; Gruszczynski et al. 2008; Baldassini and Di Stefano 2015 and reference therein). These deeply investigated surfaces are commonly related to sea-level low-stand (Pedley and Bennett 1985; Rose et al. 1992; Rehfeld and Janssen 1995; Gruszczynski et al. 2008; Baldassini and Di Stefano 2015), while the overlying phosphatic beds have been interpreted as condensed intervals, often followed by new sea-level shallowing as testified by their common planar top (Baldassini and Di Stefano 2015 and reference therein).

Following Baldassini and Di Stefano (2015) who compared the depositional intervals of the GLF to those recognized by Boulila et al. (2011) in the New Jersey passive margin, a geodynamic setting comparable to that characterizing the deposition of the Maltese sequences, we attempted the same approach to the entire sedimentary succession. In fact, the analogy of the depositional context, mostly driven by eustatic fluctuations in an almost tectonically stable foreland environment, makes the situations alike, with normal sedimentation processes interrupted by unconformities reflecting insolation minima within 1.2 Myrs long obliquity cycles and often associated to hiatuses (Miller et al. 1998; Steckler et al. 1999; Boulila et al. 2011). In this setting, it is possible to hieratically frame these sequences within the third-order cycles (Boulila et al. 2011; Baldassini and Di Stefano 2015).

5.1 Lower Coralline Limestone Formation

Brandano et al. (2009a, b) recognized the third-order sea-level fluctuations as the most important responsible for the stratigraphic architecture of the Attard Member (LCLF), chronostratigraphically framing the member to the early Chattian (between the sequence boundaries Ru4/Ch1 and Ch2 of Hardenbol et al. 1998). By combining this interpretations with the sequence stratigraphic data of Boulila et al. (2011), constrained by the biostratigraphic attribution of the overlying members, it is possible to tentatively associate the depositional interval of the Attard Mb to the sequence O4 of Boulila et al. (2011), which embraces the time interval between 27.9 and 27.1 Ma (late Chattian, late Oligocene) (Fig. 6).

The heteropic Il-Mara and Xlendi members (LCLF) are characterized by well-evident unconformities both at their base and at top. Because of the lack of biostratigraphic indicative fossils, these deposits can only be indirectly ascribed to the middle Chattian (late

Oligocene) through the comparison with the underlying and overlying members, and can be correlated to the O5 sequence, framed between 26.9 and 25.7 Ma (Fig. 6).

It is therefore possible to recognize a sedimentary hiatus between the Attard Mb and the Il-Mara/Xlendi Mb, which realized between 27.1 and 26.9 Ma, covering a time interval of at least 200 Kyrs (Fig. 6).

According to Baldassini et al. (2013), the LGLM throughout the entire archipelago is framed within the upper part of the nannofossil MNP25a Zone and the middle part of the Foraminifera P22 Zone, and thus between 25.1 and 24.3 Ma in age. This chronological framing is coherent with the sequence O6 of Boulila et al. (2011), dated between 25.5 and 24.3 Ma (Fig. 6).

The sedimentary hiatus occurring between the LCLF and the GLF has duration of no less than 600 Kyrs, being framed between 25.7 and 25.1 Ma (Fig. 6).

5.2 Globigerina Limestone Formation

As shown above, the MGLM is characterized by different depositional intervals both in the Maltese and Gozitan outcrops (Figs. 5, 6). Specifically, the member displays a latest Chattian (late Oligocene) age at Il Blata (western coast of Malta Island), being ascribed to the calcareous nannofossil MNN1b Subzone and to the uppermost part of the planktonic Foraminifera P22 Zone. This bio-chronostratigraphic attribution allows a good correlation with the uppermost part of the O7 sequence of Boulila et al. (2011), dated between 24.3 and 21.99 Ma (Fig. 6). In the same area, the member exhibits a late Aquitanian deposition supported by the biostratigraphic attribution to the calcareous nannofossil MNN1d Subzone and to the lower part of the planktonic Foraminifera MMi2b Subzone, which well fits with the Kw1a sequence, dated between 21.2 and 20.99 Ma (Fig. 6). In the Delimara section, along the southeastern coast of Malta Island, the deposits have been attributed to the calcareous nannofossil MNN2b–MNN4a (lower–middle portion) and to the planktonic Foraminifera MMi2b–MMi2c zones (between about 19.7 and 17.2 Ma), allowing the correlation to the Kw1c–Kw2b (intermediate portion) sequences that embraces a time interval spanning between 19.78 and 16.48 Ma (Fig. 6).

At Il Blata and Qammieh (western and northern coast of Malta Island), and Xatt L-Ahmar (along the southern coast of Gozo Island), the MGLM has been framed within the MNN3a Zone, while at Fomm ir-Rih Bay (along the western coast of Malta Island) and at Dabrani and Xwieni Bay sections (northern part of Gozo Island), within the MNN3b Zone. This ascription allows attributing these middle Burdigalian deposits to the Kw2a sequence (Fig. 6). Specifically, the older deposits can be correlated to the lower–middle part of this sequence, whereas the younger deposits to its middle-upper part (Fig. 6).

The sedimentary hiatus occurring between the LGLM and the MGLM shows therefore different durations in the various areas of the archipelago (Fig. 6). Specifically, along the western coast of Malta Island (Il Blata section), this latter hiatus spans between 24.3 and 23.38 Ma (FO of *Sphenolithus delphix*; Table 3) for an overall duration of at least 900 Kyrs, while the hiatus between the early and late Aquitanian deposits covers an interval of no less than 1.86 Myrs, between 23.06 Ma (LO of *S. delphix*; Table 3) and 21.2 Ma (Fig. 6). The sedimentary hiatus separating the Aquitanian and the Burdigalian deposits in this area has a duration of about 1.93 Myrs, occurring between 20.99 and 19.06 Ma (Fig. 6).

In the southern part of Malta Island (Delimara section), the hiatus between the lower and intermediate members of the GLF covers a time interval at least of 4.5 Myrs (between 24.3 and 19.78 Ma), while in the northern part of the island (Qammieh section) and in the

southern of Gozo Island (Xatt L-Ahmar section), it spans for 5.24 Myrs, depicting a time interval between 24.3 and 19.06 Ma (Fig. 6). Furthermore, in the Dabrani and Xwieni Bay sections (northern part of Gozo Island) the hiatus embraces as a minimum 5.87 Ma, being framed between 24.3 and 18.43 Ma (LCO of *Sphenolithus belemnos*; Table 3).

The oldest deposits belonging to the UGLM are recovered at Delimara section and were attributed to the nannofossil MNN4a–MNN5a (lowermost part) interval zone and to the Foraminifera MMi3–MMi4c, dated between 16.48 and about 15.3 Ma. This interval of deposition is comparable with the New Jersey sequence Kw2c (16.06–15.58 Ma), although in this part of the Maltese Archipelago, it is characterized by a greater duration (Fig. 6). At Il Blata the oldest deposits of the UGLM have been deposited within the calcareous nannofossil MNN4b Subzone and planktonic Foraminifera MMi4a Subzone, between 16.05 Ma (LCO of *Helicosphaera ampliaperta*; Table 3) and 15.64 Ma (PB of *S. heteromorphus*; Table 3) and has been compared to the Kw2c sequences that embrace the time interval between 16.06 and 15.58 Ma (Fig. 6).

The youngest deposits of the UGLM at Il Blata, as well as at Fomm ir-Rih and Xwieni Bay, have been ascribed to the MNN5a–MNN5c and MMi4c (uppermost part)–MMi5b biozonal intervals, displaying a depositional age spanning between about 15 and 13.82 Ma (Fig. 6). This deposition interval can be correlated to the lower–middle portion of the Kw3 sequence corresponding to the time interval among 14.67 and 12.94 Ma (Fig. 6). Deposits belonging to this member in Malta (Karraba and Qammieh) and Gozo (Xatt L-Ahmar and Dabrani) have been ascribed to the MNN5a (uppermost part)–MNN5c (lowermost part) and to the MMi4d–MMi5b biozonal intervals, covering an age comprised between 14.89 and 13.82 Ma, and well fitting with the lower–middle portion of sequence Kw3 (Fig. 6).

The sedimentary hiatus among the intermediate and upper members of the GLF displays its minimum duration in the southern part of the Malta Island (Delimara section), where it embraces at least 720 Kyrs, between 17.2 and 16.48 Ma, and at Il Blata section where it spans between 18.43 and 16.06 Ma, covering no less than 2.37 Myrs (Fig. 6). The hiatus between the older and the younger UGLM deposits at Il Blata has a duration of at least 410 Kyrs, being comprised between 15.64 and 15.23 Ma (Fig. 6). Along the western coast of Malta Island (Fomm ir-Rih section) and the northern sector of Gozo (Xwieni Bay section), the hiatus embraces at least 2.76 Myrs, spanning between 17.99 and 15.23 Ma (Fig. 6), while in the Dabrani section (northern part of Gozo), it straddles between 17.99 and 14.89 Ma, displaying a duration of no less than 3.1 Myrs (Fig. 6). At the Qammieh and the Xatt L-Ahmar sections, the hiatus between MGLM and UGLM is comprised between 18.43 and 14.89 Ma, exhibiting a sedimentation lag of at least 3.54 Myrs (Fig. 6).

5.3 Blue Clay Formation

The depositional interval of BCF from the base to the unconformity surface in its uppermost layers (Fig. 5) is framed, at Fomm ir-Rih Bay, within the MNN5c–MNN7a (calcareous nannofossil) and MMi5c–MMi7b (planktonic Foramiinifera) biozones, highlighting an age between 13.82 and about 12.4 Ma, and corresponding to the middle-upper portion of the sequence Kw3 (14.67–12.94 Ma), the Kw-Ch1 (12.94–12.75 Ma;) and the lowermost part of the Kw-Ch2 (12.53–11.58 Ma) of Boulila et al. (2011) (Fig. 6). At Karraba section, the sedimentation stops within the planktonic foraminiferal Subzone MMi7a, restricting the deposition interval between 13.82 and about 12.5 Ma, and allowing a comparison with the sequences Kw3 and Kw-Ch1 (Fig. 6). The BCF outcropping at Gozo Island (Dabrani and Xwieni Bay sections) are characterized by a further reduction in

deposition being framed within the calcareous nannofossil MNN5c–MNN6b zones (between 13.82 and about 12.6 Ma) and reflecting the sequences Kw3 and Kw-Ch1 (Fig. 6).

The youngest layers of the BCF have been framed within the calcareous nannofossil MNN8a–MNN8b zones and the planktonic Foraminifera MMi10–MMi11 zones, embracing a time span between 10.76 and 10.49 Ma that does not allow a direct correlation with the New Jersey sequences (Fig. 6).

The duration of sedimentary hiatuses recognizable within the deposits of the BCF increase northwards, being at least 1.64 Myrs (between about 12.4 and 10.76 Ma) at Fomm ir-Rih, 1.74 Myrs at Karraba (between 12.5 and 10.76 Ma), and 1.84 Myrs (between 12.6 and 10.76 Ma) at Dabrani and Xwieni Bay sections (Fig. 6).

5.4 Greensand and Upper Coralline Limestone formations

The GSF is attributed to the nannofossil MNN11a Zone and deposited between 8.80 and 7.39 Ma. This interval can be correlated (also due to its stratigraphic position with respect to the overlying UCLF) to the sequence Kw-Ch5, developed between 8.66 and 8.23 Ma (Fig. 6). This latter attribution allows recognizing a depositional hiatus between the BCF and the GSF of at least 1.83 Myrs (between 10.49 and 8.66 Ma) in all the considered areas (Fig. 6).

The UCLF, represented in the Malta outcrops (Fomm ir-Rih Bay and Karraba sections) by the Mtarfa Mb and the Tal-Piktal Mb, and in the Gozo outcrops (Dabrani and Xwieni Bay sections) by the Ghajn Melel Mb and the Tal-Piktal Mb, has been ascribed to the nannofossil zones MNN11a–MNN11b chronologically framed between 8.80 and 6.82 Ma (Fig. 6). This depositional interval could be correlated to the sequence Kw-Ch6 whose base is defined to 8.04 Ma (Boulila et al. 2011). However, the occurrence in the eccentricity curve of Boulila et al. (2011), of a well-evident minimum roughly dated to 7 Ma, allowed us to tentatively link the depositional interruption to this early Messinian orbital phase (Fig. 6).

Finally, the hiatus recorded between the GSF and the UCLF in the Maltese Archipelago occurred between 8.23 and 8.04 Ma, displaying duration of at least 190 Kyrs (Fig. 6).

6 Correlation between the Maltese deposits and the global $\delta^{18}O$ isotope events

In order to verify the role of the eustatic fluctuations during the deposition of the Maltese succession, we compared the detected sedimentation intervals (Figs. 5, 6) to a composite Oligo–Miocene global oxygen isotope curve (Kouwenhoven et al. 2003; Pekar and De Conto 2006; Boulila et al. 2011; Westerhold et al. 2011). This also resulted in a more precise definition of the sedimentary hiatuses associated to the recognized unconformities (Figs. 5, 6), which according to our reconstruction are the response to low-stand phases associated to global cooling events.

The deposits of the Attard Mb (LCLF) record a main regressive phase (Brandano et al. 2009b) culminating with the interruption of sedimentation very likely forced by the cold Oi2b event (Miller et al. 1991, 1998; Fig. 7). The subsequent transgression gave rise to the deposition of the youngest sediments of the LCLF, namely the Il-Mara and Xlendi members, whose deposition was stopped by the sea-level lowering associated with the Oi2c cooling peak (Miller et al. 1991, 1998; Fig. 7).

The deposition of the LGLM occurred during the late Chattian Stage and has been interrupted almost uniformly throughout the Maltese Archipelago by the sea-level lowering linked to the last Oligocene cold event (Oi2d, Pälike et al. 2006) (Fig. 7). This interpretation is supported by the results provided by Baldassini and Di Stefano (2015) who identified for the youngest layers of the member a shallow-water environment documented by the presence at Qammieh, of both *Lithophaga* bores and *Ostrea* specimens. In the Malta Island, and in particular along the western coast (Il Blata section) that was probably characterized by a more distal position within the depositional basin (Baldassini and Di Stefano 2015), a latest Oligocene deposition for the MGLM was observed, which was likely stopped by the setting of the Mi1 event (Fig. 7). Furthermore, the authors highlighted in the same area, the occurrence of a latest Aquitanian (early Miocene) deposition for the member, apparently interrupted by the sea-level lowering linked to the Mi1a cooling event (Fig. 7).

In the southern part of the Malta Island, the base of the MGLM is slightly older (early Burdigalian), with respect to other areas of the archipelago, probably due to a more distal position within the depositional basin. Specifically, in the Delimara section, the sedimentation process starts during the sea-level rise linked to the transgression immediately following the Mi1aa cooling event (Miller et al. 1991, 1998) (Fig. 7).

The oscillations related to the middle to late Burdigalian Mi1ab and Mi1b cooling events (Miller et al. 1991, 1998) have no direct effects on the deposition processes in the Delimara area, confirming the presence of a relatively deep sedimentation environment, at least up to the late Burdigalian, when a likely combination between the eustatic fluctuation (triggered by the Mi1b event), and a stronger tectonic activity recorded during this time interval (Grasso et al. 1994), took place interrupting the sedimentation (Fig. 7).

In other outcrops both in Malta and Gozo, probably due to the more marginal position within the depositional basin, the deposition of the MGLM is limited to the middle Burdigalian being linked to sea-level rising phases following the Mi1aa event (Figs. 6, 7).

At Il Blata and Qammieh (Malta), and at Xatt L-Ahmar (Gozo), the interruption of the sedimentation is forced by the cooling trend culminating in the Mi1ab and almost coinciding with the calcareous nannofossils MNN3a–MNN3b zonal boundary (Figs. 5, 6, 7). At Fomm ir-Rih Bay section (Malta) and Dabrani and Xwieni Bay sections (Gozo), the sedimentation starts during the transgressive phase immediately following the Mi1ab events and interrupts as consequence of the of the sea-level drop linked to the regressive phase culminating in the Mi1b (Figs. 6, 7).

Also the UGLM displays diachronous bases with its oldest deposits outcropping in the southern part of the archipelago. Specifically, in the Delimara section, the UGLM starts to deposit during a late Burdigalian sea-level high-stand, and due to its distal position within the depositional basin, is apparently not affected by the sea-level fall forced by the Mi2 cooling event, being instead interrupted probably by a combination of sea-level deep fluctuations (Fig. 7) and active tectonism (Grasso et al. 1994), during the early Langhian (middle Miocene) (Fig. 7).

In the sections of Il Blata and Fomm ir-Rih (and maybe Karraba) at Malta, and in that of Xwieni Bay at Gozo, the deposition of the UGLM starts in the middle Langhian (Figs. 5, 6), during the first transgressive phases following the Mi2a event (Miller et al. 1991, 1998; Fig. 7). Conversely, at Qammieh (Malta) and at Xatt L-Ahmar and Dabrani (Gozo) sections, the beginning of the deposition occurs during a further younger transgressive phase following the Mi2a event (Miller et al. 1991, 1998; Fig. 7).

Both in Malta and Gozo, the transition between GLF and BCF is isochronous and defined by a well-recognizable transitional bed (Fig. 4), which results from the

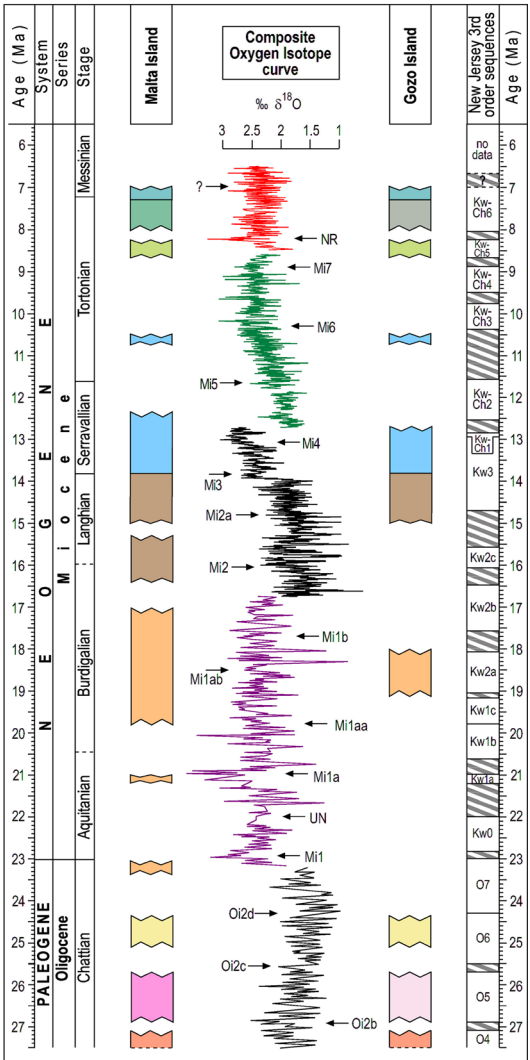

δ18O Event	δ18O Maximum Age	
Mi7	8.7 Ma	
Mi6	10.3 Ma	Boulila et al. (2011)
Mi5	11.7 Ma	
Mi4	13.2 Ma	Westerhold et al. (2005)
Mi3	13.7 Ma	
Mi2a	14.8 Ma	Boulila et al. (2011)
Mi2	16.1 Ma	
Mi1b	17.7 Ma	
Mi1ab	18.7 Ma	
Mi1aa	19.8 Ma	
Mi1a	21.0 Ma	Miller et al. unpublished, in Boulila et al. (2011)
UN	22.0 Ma	
Mi1	23.1 Ma	
Oi2d	24.3 Ma	
Oi2c	25.1 Ma	Boulila et al. (2011)
Oi2b	26.4 Ma	

Fig. 7 Comparison between the composite depositional intervals recognized on Malta and Gozo islands, and the main Oligo–Miocene cooling events of Miller et al. (1991, 1998). Composite global oxygen isotope curve after: (*black lines*) Boulila et al. (2011); (*purple line*) Pekar and De Conto (2006); (*green line*) Westerhold et al. (2011); (*red line*) Kouwenhoven et al. (2003)

environmental change triggered by the middle Miocene Mi3 cooling event (Miller et al. 1991, 1998; Fig. 7). The BCF deposited during a global cooling trend which follows this latter event and was interrupted, at Gozo Island, by the cooling trend leading to the Mi4 event of Miller et al. (1991, 1998) (Fig. 7). The deposition of BCF continued also up to late Serravallian and was stopped by a cooling phase following the Mi4 event (Fig. 7). The youngest deposits of the BCF are strongly linked to the regressive phase that led to the Mi6 (Fig. 7) cooling event of Miller et al. (1991, 1998). According to Pedley (1978), the sea-level fall during the early Tortonian time interval could have forced the erosion of phosphatic and glauconitic seamounts located northwest of the archipelago, driving the accumulation of sediments in the area.

The sediment starving persisted in the Maltese area at least until the middle Tortonian (late Miocene), when the deposition started again, giving rise to the GSF, as response to the sea-level rise linked to a transgressive phase following the Mi7 cooling event (Miller et al. 1998; Fig. 7). The deposition of the GSF stopped because of the setting of a strong regressive phase culminating in the late Tortonian NR cooling event of Boulila et al. (2011).

The deposition of the youngest sediments of the Maltese succession, belonging to the shallow-water UCLF, realized uniformly throughout the archipelago and started during the transgressive phase following the NR event. The transitions between the Mtarfa Mb and the Tal-Piktal Mb on Malta Island, and between the Ghajn Melel Mb and the Tal-Piktal Mb on Gozo Island (Figs. 5, 6, 7), occurred during the latest Tortonian-earliest Messinian time interval and are probably linked to a shallowing in the water column (Fig. 7) (Pedley 2011).

7 Conclusions

The large amount of biostratigraphic data concerning the late Oligocene–late Miocene Maltese Archipelago succession allowed a detailed definition of the sedimentary intervals, interrupted by a number of hiatuses, as response to a combination of tectonics and eustatic fluctuations, in the framework of the Central Mediterranean region.

Several sections, characterized by excellent exposures and rich fossiliferous content were investigated, outcropping both in Malta and Gozo islands, representative of the whole succession.

Geodynamic analogies between the Maltese depositional environment and the Oligo–Miocene third-order sequences of the New Jersey passive margin were recognized. Accordingly, the sedimentation intervals and the hiatuses in correspondence of the erosional surfaces or phosphate horizons were even better evaluated.

Diverse durations of the sedimentary intervals, and of the associated hiatuses, were highlighted in the different sections: for instance the hiatus between the LGLM and the MGLM embraces in Malta at least 0.9 Myrs along the western coast, and 4.5 Myrs in the southeastern coast, while at Gozo, the depositional hiatus has a duration of at least 5.24 Myrs long. In the same way, the hiatus between the MGLM and UGLM is characterized by its minimum duration along the southeastern coast of Malta where it embraces 0.72 Myrs, and by its maximum along the northern coast of Malta and southern of Gozo, where it spans for 3.54 Myrs. Furthermore, some intraformational lacunas were also detected both within the MGLM and UGLM. The sedimentary hiatus recognized within the BCF is

characterized by different duration in the archipelago, being 1.64 Myrs along the western coast of Malta, and 1.84 Myrs in the northern sector of Gozo.

The diachronies at the base of the MGLM and the UGLM, as well as that at the top of the BCF, have been related to different positions of the succession (distal vs. marginal) within the sedimentary basin, emphasized by tectonics.

Finally, the opportunity to compare the investigated succession with a composite oxygen isotope curve allows connecting the sedimentation interruptions with the low-stand phases associated to global cooling events, and the depositional intervals to the high-stand stages linked to global warming events.

Acknowledgments This work has been financially supported and carried out within the P.O. Italia-Malta 2007–2013 *SIMIT* Project "Constitution of an integrated Italy–Malta system of civil protection", Scientific Responsible of Project Partner 3 (University of Catania): Agata Di Stefano, and within the "PRIN2012" project "The Burdigalian GSSP (Global Stratigraphic Section and Point): the missing tile to complete the Neogene interval of the Geological Time scale", financed by the Italian MIUR and coordinated by Agata Di Stefano. The authors warmly thank two anonymous reviewers for their constructive suggestions and are indebted with Giovanni Barreca for his help in realizing the digitalization of the map shown in Fig. 1.

References

Abdul Aziz A, Di Stefano A, Foresi LM, Hilgen FJ, Iaccarino SM, Kuiper KF, Lirer F, Salvatorini G, Turco E (2008) Integrated stratigraphy and 40Ar/39Ar chronology of early Middle Miocene sediments from DSDP Leg 42A, Site 372 (Western Mediterranean). Palaeogeogr Palaeoclimatol Palaeoecol 257:123–138

Abels HA, Hilgen FJ, Krijgsman W, Kruk RW, Raffi I, Turco E, Zachariasse WJ (2005) Long-period orbital control on middle Miocene global cooling: integrated stratigraphy and astronomical tuning of the Blue Clay Formation on Malta. Paleoceanography 20(4):PA4012. doi:10.1029/2004PA001129

Agnini C, Fornaciari E, Raffi I, Catanzariti R, Pälike H, Backman J, Rio D (2014) Biozonation and biochronology of Paleogene calcareous nannofossils from low and middle latitudes. Newsl Stratigr 47(2):131–181. doi:10.1127/0078-0421/2014/0042

Backman J, Raffi I, Rio D, Fornaciari E, Pälike H (2012) Biozonation and biochronology of Miocene through Pleistocene calcareous nannofossils from low and middle latitudes. Newsl Stratigr 45(3):221–244. doi:10.1127/0078-0421/2012/0022

Baldassini N (2012) Biostratigraphy of the Oligo–Miocene Globigerina Limestone Formation (Maltese Archipelago) based on calcareous nannofossils. Ph.D. thesis, University of Siena, Italy

Baldassini N, Di Stefano A (2015) New insights on the Oligo–Miocene succession bearing phosphatic layers of the Maltese Archipelago. Ital J Geosci 134(2):355–366. doi:10.330/IJG.2014.52

Baldassini N, Mazzei R, Foresi LM, Riforgiato F, Salvatorini G (2013) Calcareous plankton bio-chronostratigraphy of the Maltese Lower Globigerina Limestone Member. Acta Geol Pol 63(1):105–135. doi:10.2478/agp-2013-0004

Berggren WA, Kent DV, Swisher CC III, Aubry M-P (1995) A revised cenozoic geochronology and chronostratigraphy. In: Berggren WA, Kent DV, Aubry M-P, Hardendol J (eds) Geochronology, time scales and global stratigraphic correlation, vol 54. SEPM Special Publication, Tulsa, pp 129–212

Bianucci G, Gatt M, Catanzariti R, Sorbi S, Bonavia CG, Curmi R, Varola A (2011) Systematics, biostratigraphy and evolutionary patterns of the Oligo–Miocene marine mammals from the Maltese Islands. Geobios 44(6):549–585. doi:10.1016/j.geobios.2011.02.009

Biolchi S, Furlani S, Antonioli F, Baldassini N, Deguara JC, Devoto S, Di Stefano A, Evans J, Gambin T, Gauci R, Mastronuzzi G, Monaco C, Scicchitano G (2016) Boulder accumulations related to extreme wave events on the eastern coast of Malta. Nat Hazard Earth Syst Sci 16:737–756. doi:10.5194/nhess-16-737-2016

Blow WH (1969) Late Middle Eocene to Recent Planktonic foraminiferal biostratigraphy. In: Brönnimann P, Renz HH (eds) Proceedings of the first international. Conference on planktonic microfossils, Geneva, pp 199–421

Boulila S, Galbrun B, Miller KG, Pekar SF, Browning JV, Laskar J, Wright JD (2011) On the origin of Cenozoic and Mesozoic "third-order" eustatic sequences. Earth Sci Rev 109(3):94–112. doi:10.1016/j.earscirev.2011.09.003

Brandano M, Frezza V, Tomassetti L, Cuffaro M (2009a) Heterozoan carbonates in oligotrophic tropical waters: the Attard member of the lower coralline limestone formation (Upper Oligocene, Malta). Palaeogeogr Palaeoclimatol Palaeoecol 274:54–63. doi:10.1016/j.palaeo.2008.12.018

Brandano M, Frezza V, Tomassetti L, Pedley HM, Matteucci R (2009b) Facies analysis and palaeoenvironmental interpretation of the late Oligocene Attard Member (Lower Coralline Limestone Formation), Malta. Sedimentology 56:1138–1158. doi:10.1111/j.1365-3091.2008.01023.x

Carbone S, Grasso M, Lentini F, Pedley HM (1987) The distribution and paleoenvironment of early Miocene phosphorites of southeast Sicily and their relationship with the Maltese phosphorites. Paleogeogr Palaeoclimatol Palaeoecol 58:35–53

Carminati E, Doglioni C (2005) Mediterranean tectonics. In: Selley RC, Cocks LMR, Plimer IR (eds) Encyclopedia of geology, vol 2. Elsevier, Amsterdam, pp 135–146

Catalano S, De Guidi G, Lanzafame G, Monaco C, Tortorici L (2009) Late Quaternary deformation on the island on Pantelleria: new constraints for the recent tectonic evolution of the Sicily Channel Rift (southern Italy). J Geodyn 48:75–82. doi:10.1016/j.jog.2009.06.005

Cavallaro D, Monaco C, Polonia A, Sulli A, Di Stefano A (2016) Evidence of positive tectonic inversion in the north-central sector of the Sicily Channel. Nat Hazards (under review)

Cita MB, Fantini Sestini N, Salvatorini G, Mazzei R, Kidd RB (1979) Late Neogene sediments and fossils from the Malta Escarpment and their geodynamic significance. Ann Géol Hell 1:273–283

Corti G, Cuffaro M, Doglioni C, Innocenti F, Manetti P (2006) Coexisting geodynamic processes in the Sicily Channel. In: Dilek Y, Pavlides S (eds) Postcollisional tectonics and magmatism in the Mediterranean region and Asia. Geological Society of America Bulletin, Spec. Paper 409, pp 83–96

Dart CJ, Bosence WJ, McClay KR (1993) Stratigraphy and structure of the Maltese graben system. J Geol Soc Lond 150:1153–1166

De Guidi G, Lanzafame G, Palano M, Puglisi G, Scaltrito A, Scarfi' L (2013) Multidisciplinary study of the Tindari Fault (Sicily, Italy) separating ongoing contractional and extensional compartments along the active Africa–Eurasia convergent boundary. Tectonophysics 588:1–17. doi:10.1016/j.tecto.2012.11.021

Di Stefano A (1993) Contributo alla biostratigrafia a nannofossili calcarei del Miocene dell'area Mediterranean. Analisi di sequenze mioceniche attraverso l'orogene centro-mediterraneo. Ph.D. thesis, University of Catania, Italy

Di Stefano A, Foresi LM, Lirer F, Iaccarino SM, Turco E, Amore FO, Mazzei R, Morabito S, Salvatorini G, Abdul Aziz H (2008) Calcareous plankton high resolution bio-magnetostratigraphy for the Langhian of the Mediterranean area. Riv Ital Paleontol Stratigr 114:51–76

Di Stefano A, Verducci M, Cascella A, Iaccarino SM (2011) Calcareous plankton events at the Early/Middle Miocene transition of DSDP Hole 608: comparison with Mediterranean successions for the definition of the Langhian GSSP. Stratigraphy 8(2-3):145–161

Felix R (1973) Oligo–Miocene stratigraphy of Malta and Gozo. Meded Landbouwhogesch Wagening 73:1–104

Finetti I (1984) Geophysical study of the Sicily Channel Rift Zone. Boll Geofis Teorica Ed Appl 26(101–102):3–27

Föllmi KB, Gertsch B, Renevey J-P, De Kaenel E, Stilles P (2008) Stratigraphy and sedimentology of phosphate-rich sediments in Malta and south-eastern Sicily (latest Oligocene to early Late Miocene). Sedimentology 55:1029–1051. doi:10.1111/j.1365-3091.2007.00935.x

Foresi LM, Bonomo S, Caruso A, Di Stefano E, Salvatorini G, Sprovieri R (2002) Calcareous plankton biostratigraphy (Foraminifera and nannofossils) of the uppermost Langhian—lower SerravallianRas il-Pellegrin Section (Malta). Riv Ital Paleontol Stratigr 108(2):195–210

Foresi LM, Mazzei R, Salvatorini G, Donia F (2008) Biostratigraphy and chronostratigraphy of the Maltese Lower Globigerina Limestone Member (Globigerina Limestone Formation): new preliminary data based on calcareous plankton. Boll Soc Paleontol Ital 46(2–3):175–181

Foresi LM, Verducci M, Baldassini N, Lirer F, Mazzei R, Salvatorini G, Ferraro G, Da Prato S (2011) Integrated stratigraphy of St. Peter's Pool section (Malta): new age for the Upper Globigerina Limestone Member and progress towards the Langhian GSSP. Stratigraphy 8:125–143

Foresi LM, Baldassini N, Sagnotti L, Lirer F, Di Stefano A, Caricchi C, Verducci M, Salvatorini G, Mazzei R (2014) Integrated stratigraphy of the St. Thomas section (Malta Island): a reference section for the lower Burdigalian of the Mediterranean Region. Mar Micropaleontol 111:66–89. doi:10.1016/j.marmicro.2014.06.004

Fornaciari E, Rio D (1996) Latest Oligocene to early middle Miocene quantitative calcareous nannofossil biostratigraphy in the Mediterranean region. Micropaleontology 42(1):1–36

Fornaciari E, Di Stefano A, Rio D, Negri A (1996) Middle Miocene quantitative calcareous nannofossil biostratigraphy in the Mediterranean region. Micropaleontology 42:37–63

Giannelli L, Salvatorini G (1972) I Foraminiferi planctonici dei sedimenti terziari dell'Arcipelago Maltese. Biostratigrafia del "Globigerina Limestone" I. Atti Soc Toscana Sci Nat Mem Ser A 79:49–74

Giannelli L, Salvatorini G (1975) I Foraminiferi planctonici dei sedimenti terziari dell'Arcipelago Maltese. Biostratigrafia di "Blue Clay", "Greensand" and "Upper Coralline Limestone" II. Atti Soc Toscana Sci Nat Mem Ser A 82:1–24

Grasso M, Pedley HM (1985) The Pelagian Islands: a new geological interpretation from sedimentological and tectonic studies and its bearing on the evolution of the Central Mediterranean (Pelagian Block). Geol Romana 24:13–24

Grasso M, Pedley HM, Reuther CD (1985) The geology of the Pelagian Islands and their structural setting related to the Pantelleria rift (Central Mediterranean sea). Centro 1(2):1–19

Grasso M, Pedley HM, Maniscalco R (1994) The application of a late Burdigalian early Langhian highstand event in correlating complex Tertiary orogenic carbonate successions within the central Mediterranean. Geol Méditerr 21(1–2):69–83

Gruszczynski M, Marshall JD, Goldring R, Coleman ML, Malkowski L, Gazdzicka E, Semil J, Gatt P (2008) Hiatal surfaces from the Miocene Globigerina Limestone Formation of Malta: biostratigraphy, sedimentology, trace fossils and early diagenesis. Palaeogeogr Palaeoclimatol Palaeoecol 270(2–3):239–251

Gueguen E, Doglioni C, Fernandez M (1998) On the post 25 Ma geodynamic evolution of the western Mediterranean. Tectonophysics 298:259–269. doi:10.1016/S0040-1951(98)00189-9

Hardenbol J, Thierry J, Farley MB, Jacquin T, De Graciansky P-C, Vail P (1998) Mesozoic and Cenozoic sequence chronostratigraphic framework of European basins. In: Mesozoic and Cenozoic sequence chronostratigraphic framework of European basins. In: De Graciansky P-C, et al. (eds) Society for Sedimentary Geology (SEPM) Special Publication 60, Chapter 1

Hilgen FJ, Abdul Aziz H, Krijgsman W, Raffi I, Turco E (2003) Integrated stratigraphy and astrochronology of the Serravallian and lower Tortonian at Monte dei Corvi (Middle-Upper Miocene, Northern Italy). Palaeogeogr Palaeoclimatol Palaeoecol 199:229–264

Hilgen FJ, Abels HA, Iaccarino SM, Krijgsman W, Raffi I, Sprovieri R, Turco E, Zachariasse WJ (2009) The global stratotype section and point (GSSP) of the Serravallian Stage (Middle Miocene). Episodes 32:152–166

Holbourn A, Kuhnt W, Schulz M, Flores JA, Andersen N (2007) Orbitally-paced climate evolution during the middle Miocene "Monterey" carbon-isotope excursion. Earth Planet Sci Lett 261(3):534–550. doi:10.1016/j.epsl.2007.07.026

Huesing SK, Hilgen FJ, Abdul Aziz H, Krijgsman W (2007) Completing the Neogene geological time scale between 8.5 and 12.5 Ma. Earth Planet Sci Lett 253:340–358

Hüsing SK, Cascella A, Hilgen FJ, Krijgsman W, Kuiper KF, Turco E, Wilson D (2010) Astrochronology of the Mediterranean Langhian between 15.29 and 14.17 Ma. Earth Planet Sci Lett 290:254–269. doi:10.1016/j.epsl.2009.12.002

Iaccarino SM, Salvatorini G (1982) A framework of planktonic foraminiferal biostratigraphy for Early Miocene to late Pliocene Mediterranean area. Paleontol Stratigr Evol 2:115–125

Iaccarino SM, Premoli Silva I, Biolzi M, Foresi LM, Lirer F, Turco F, Petrizzo MR (2007) Practical manual of Neogene planktonic Foraminifera. In: Biolzi M, Iaccarino SM, Turco E, Checconi A, Rettori R (eds) Neogene Planktonic Foraminifera, International School on Planktonic Foraminifera, Perugia, Italy

Iaccarino SM, Di Stefano A, Foresi LM, Turco E, Baldassini N, Cascella A, Da Prato S, Ferraro L, Gennari R, Hilgen FJ, Lirer F, Maniscalco R, Mazzei R, Riforgiato F, Russo B, Sagnotti L, Salvatorini G, Speranza F, Verducci M (2011) High-resolution integrated stratigraphy of the Mediterranean Langhian: comparison with the historical stratotype and new perspectives for the GSSP. Stratigraphy 8(2–3):199–215

Jacobs E, Weissert H, Shield G, Stille P (1996) The Monterey event in the Mediterranean: a record from shelf sediments of Malta. Palaeogeogr Palaeoclimatol Palaeoecol 11(6):717–728

John CS, Mutti M, Adatte T (2003) Mixed carbonate-siliciclastic record on the North African margin (Malta)—coupling of weathering premesse and mid Miocene climate. Geol Soc Am Bull 115(2):217–229. doi:10.1130/0016-7606(2003)115<0217:MCSROT>2.0.CO;2

Kienel U, Rehfeld U, Bellas SM (1995) The Miocene Blue Clay formation of the Maltese Islands: sequence stratigraphic and paleoceanographic implications based on calcareous nannofossil stratigraphy. Berl Geowiss Abh 16:533–557

Kouwenhoven TJ, Hilgen FJ, van der Zwaan GJ (2003) Late Tortonian—early Messinian stepwise disruption of the Mediterranean–Atlantic connections: constraints from benthic foraminiferal and geochemical data. Palaeogeogr Palaeoclimatol Palaeoecol 198(3–4):303–319. doi:10.1016/S0031-0182(03)00472-3

Kürschner MW, Kvacek Z, Dilcher DL (2008) The impact of Miocene atmospheric carbon dioxide fluctuations on climate and the evolution of terrestrial ecosystems. Proc Natl Acad Sci USA 105(2):449–453. doi:10.1073/pnas.0708588105

Lourens L, Hilgen F, Shackleton NJ, Laskar J, Wilson D (2004) The Neogene Period. In: Gradstein F, Ogg J, Smith A (eds) A geological timescale 2004. Cambridge University Press, Cambridge, pp 409–440

Mazzei R (1986) The Miocene sequence of the Maltese Islands: biostratigraphic and chronostratigraphic references based on nannofossils. Atti Soc Toscana Sci Nat Mem Ser A 9:165–197

Miller KG, Feigenson MD, Wright J, Bradford CM (1991) Miocene isotope reference section, Deep Sea Drilling Project Site 608: an evaluation of isotope and biostratigraphic resolution. Paleoceanography 6(1):33–52. doi:10.1029/90PA01941

Miller KG, Mountain GS, Browning JV, Kominz M, Sugarman PJ, ChristieBlick N, Katz ME, Wright JD (1998) Cenozoic global sea level, sequences, and the New Jersey transect: results from coastal plain and continental slope drilling. Rev Geophys 36(4):569–601. doi:10.1029/98RG01624

Mourik AA, Abels HA, Hilgen FJ, Di Stefano A, Zachariasse WJ (2011) Improved astronomical age constrains for the Middle Miocene climate transition based on high-resolution stable isotopes records from the central Mediterranean Maltese Islands. Paleoceanography 26:PA1210. doi:10.1029/2010PA001981

Okada H, Bukry D (1980) Supplementary modification and introduction of code numbers to the low latitude coccolith biostratigraphy zonation (Bukry 1973, 1975). Mar Micropaleontol 51:321–325

Pälike H, Norris RD, Herrie JO, Wilson PA, Coxall HK, Lear CH, Shackleton NJ, Tripati AK, Wade BS (2006) The heartbeat of the Oligocene climate system. Science 314:1894–1898. doi:10.1126/science.1133822

Pedley HM (1976) A paleoecological study of the Upper Coralline Limestone Terebratula–Aphelesia Bed (Miocene, Malta) based on bryozoan growth-forms and brachiopod distribution. Palaeogeogr Palaeoclimatol Palaeoecol 20:209–234

Pedley HM (1978) A new lithostratigraphical and paleoenvironmental interpretation for the coralline limestone formations (Miocene) of the Maltese Islands. Inst Geol Sci Overseas Geol Miner Resour 54:273–291

Pedley HM (1993) Geological map of the Maltese Island: sheets 1, Malta island; sheet 2, Gozo Island. British Geological Survey. Publication of the Oil Exploration Directorate, Office of the Prime Minister, Malta

Pedley HM (2011) The Calabrian Stage, Pleistocene highstand in Malta: a new marker for unravelling the late Neogene and Quaternary history of the islands. J Geol Soc 168(4):913–926

Pedley HM, Bennett SM (1985) Phosphorites, hardgrounds and syndepositional subsidence: a paleoenvironmental model from Miocene of the Maltese Islands. Sed Geol 45:1–34

Pedley HM, Waugh B (1976) Easter field meeting to the Maltese Islands. 7–14 April 1974. Proc Geol As 87(3):343–385

Pedley HM, House MR, Waugh B (1976) The geology of Malta and Gozo. Proc Geol As 87(3):325–341

Pekar SF, De Conto RM (2006) High-resolution ice-volume estimates for the early Miocene: evidence for a dynamic ice sheet in Antarctica. Palaeogeogr Palaeoclimatol Palaeoecol 231:101–109. doi:10.1016/j.palaeo.2005.07.027

Raffi I, Mozzato C, Fornaciari E, Hilgen FJ, Rio D (2003) Late Miocene calcareous nannofossil biostratigraphy and astrobiochronology for the Mediterranean region. Micropaleontology 49(1):1–26. doi:10.2113/49.1.1

Rehfeld U, Janssen AW (1995) Development of phosphatized hardgrounds in the Miocene Globigerina Limestone of the Maltese Archipelago, including a description of *Gamopleura melitensis* sp. *novo* (Gastropoda, Euthecosomata). Facies 33:91–106

Rose EPF, Pratt SK, Bennett SM (1992) Evidence for sea-level changes in the Globigerina limestone formation (Miocene) of the Maltese Islands. Paleontol Evol 24–25:265–276

Russo A, Bossio A (1975) Prima caratterizzazione degli ostracodi per la biostratigrafia e la paleoecologia del Miocene dell'arcipelago Maltese. Boll Soc Paleontol Ital 15:215–227

Sprovieri M, Bellanca A, Neri R, Mazzola S, Bonanno A, Patti B, Sorgente R (1999) Astronomical calibration of late Miocene stratigraphic events and analysis of precessionally driven paleoceanographic changes in the Mediterranean basin. Mem Soc Geol Ital 54:7–24

Sprovieri M, Caruso A, Foresi LM, Bellanca A, Neri R, Mazzola S, Sprovieri R (2002) Astronomical calibration of the upper Langhian/lower Serravallian record of Ras Il-Pellegrin section (Malta Island, central Mediterranean). Riv Ital Paleontol Stratigr 108(2):183–193

Steckler MS, Mountain GS, Miller KG, Christie-Blick N (1999) Reconstruction of Tertiary progradation and clinoform development on the New Jersey passive margin by 2-D backstripping. Mar Geol 154(1):399–420. doi:10.1016/S0025-3227(98)00126-1

Steininger FF, Iaccarino SM (1996) Synthesis on the GSSP Lemme-Carosio section. Giornale di geologia 58(1-2):141–147

Steininger FF, Aubry M-P, Berggren WA, Biolzi M, Borsetti AM, Cartlidge JE, Cati F, Corfield R, Gelati R, Iaccarino S, Napoleone C, Ottner F, Rögl F, Roetzel R, Spezzaferri S, Tateo F, Villa G, Zevenboom D (1997) The global stratotype section and point (GSSP) for the base of the Neogene

Turco E, Cascella A, Gennari R, Hilgen FJ, Iaccarino SM, Sagnotti L (2011) Integrated stratigraphy of the La Vedova section (Conero Riviera, Italy) and implications for the Burdigalian/Langhian boundary. Stratigraphy 8(2):89–110

Vincent E, Berger WH (1985) Carbon dioxide and polar cooling in the Miocene: the Monterey hypothesis. Geophys Monogr Ser 32:455–468. doi:10.1029/GM032p0455

Wade BS, Pearson PN, Berggren WA, Pälike H (2011) Review and revision of Cenozoic tropical planktonic foraminiferal biostratigraphy and calibration to the geomagnetic polarity and astronomical time scale. Earth Sci Rev 104:111–142. doi:10.1016/j.earscirev.2010.09.003

Westerhold T, Bickert T, Röhl U (2005) Middle to late Miocene oxygen isotope stratigraphy of ODP site 1085 (SE Atlantic): new constraints on Miocene climate variability and sea-level fluctuations. Palaeogeogr Palaeoclimatol Palaeoecol 217:205–222

Westerhold T, Röhl U, Donner B, McCarren HK, Zachos JC (2011) A complete high-resolution Paleocene benthic stable isotope record for the central Pacific (ODP Site 1209). Paleoceanography 26:PA2216. doi:10.1029/2010PA002092

Woodruff F, Savin SM (1989) Miocene deepwater oceanography. Paleoceanography 4:87–140. doi:10.1029/PA004i001p00087

Woodruff F, Savin SM (1991) Mid-Miocene isotope stratigraphy in the deep-sea: high resolution correlations, paleoclimatic cycles, and sediment preservation. Paleoceanography 6:755–806

Zachos J, Pagani M, Sloan L, Thomas E, Billups K (2001) Trends, rhythms, and aberrations in global climate 65 Ma to present. Science 292(5517):686–693. doi:10.1126/science.1059412

Zachos JC, Dickens GR, Zeebe RE (2008) An early Cenozoic perspective on greenhouse warming and carbon-cycle dynamics. Science 451:279–283. doi:10.1038/nature06588